
Check for updates

in the slurry. It is not clear from the publication [8], if and how the ionomer content was changed in their experiments. Recently, Ahadi et al. [12] performed ex–situ four–probe measurements of σ_e anisotropy in self-prepared CCLs and reported the through-plane electron conductivity to be three orders of magnitude lower than the in-plane one. More references could be found in a recent review by Tang et al. [13].

In this work, we report a novel method for *in-situ* measurement of electron and proton conductivity of the CCL in the Fe-N-C-based cell. We ran the cell under the H_2/N_2 testing regime and fit a recently developed model for the CCL impedance to the measured impedance spectra. Fitting returns σ_p, σ_e, and the double layer capacitance. The electron conductivity of the studied electrodes was found to be in the range of 100 to 1000 mS cm^{-1}. Overall, the method allows one to perform simultaneous measurements of the reference proton and electron conductivity of Fe-N-C-based PEMFC cathodes.

2. Model

Following a traditional method, the cell was run under the H_2/N_2 testing regime flowing pure hydrogen and nitrogen on the anode and cathode side, respectively. It should be noted, that in contrast to Pt/C, Fe-N-C catalysts are not active towards hydrogen oxidation reaction. Measured DC current in the cell of 0.4 to 2 mA cm^{-2} could be attributed to protons produced in carbon corrosion reaction on the cathode side and consumed in hydrogen evolution reaction on the cell anode. The cell impedance is determined by charging and discharging of the double layer on the cell cathode, which includes transport of protons and electrons to/from the catalyst/electrolyte interface. Due to ten times lower thickness of the anode catalyst layer, the impedance of double layer charging and discharging on the anode side could be neglected. Note that small DC proton current in the cell eliminates contribution of bulk membrane to the double layer capacitance.

The impedance model of the oxygen-free catalyst layer used below is based on the model for PEMFC performance, which takes into account oxygen transport and finite electron conductivity of the CCL [14]. A basic equation for the CCL impedance has been derived from the transient proton, electron and oxygen conservation equations in the electrode. In the limit of zero ORR exchange current density, this model reduces to the following expression for the CCL impedance [14]:

$$Z_{CCL} = \frac{l_t}{\sigma_p}\left(\frac{(1+i)(2k+(1+k^2)\cos p)+iq\sin p}{k(iq-(1+i)p)\sin p}\right) \tag{1}$$

where i is the imaginary unit, p and q are the dimensionless parameters

$$p = \sqrt{-i\left(1+\frac{1}{k}\right)\Omega} \tag{2}$$

$$q = \sqrt{-2k(1+k)\Omega} \tag{3}$$

k is the ratio of electron σ_e to proton σ_p CCL conductivity

$$k = \frac{\sigma_e}{\sigma_p} \tag{4}$$

and Ω is the dimensionless angular frequency

$$\Omega = \frac{\omega C_{dl} l_t^2}{\sigma_p} \tag{5}$$

Here, ω is the angular frequency (s^{-1}), C_{dl} is the volumetric double layer capacitance (F cm^{-3}), and l_t is the CCL thickness. Eq. (1) describes impedance of double layer charging/discharging supported by proton keeping the [illegible] resistivity $Z_{CCL}^{\omega\to\infty}$ [14]:

$$Z_{CCL}^{\omega\to\infty} = \frac{l_t}{\sigma_p(1+k)} \tag{6}$$

Taking into account Eq. (4) and rewriting Eq. (6) as

$$\frac{1}{Z_{CCL}^{\omega\to\infty}} = \frac{1}{l_t/\sigma_p} + \frac{1}{l_t/\sigma_e} \tag{7}$$

we see that the CCL itself exhibits a "high-frequency" (ohmic) resistivity, which equals to the electronic and ionic resistivities connected in parallel. The same result has been obtained by Li and Pickup from the transmission line model of the CCL impedance [15]. From Eq. (7), it follows that if electron conductivity is large, the HF resistivity of the catalyst layer tends to zero.

Protons generated on the N_2 electrode move through the membrane, and hence the membrane proton resistivity R_m must appear in the expression for impedance. Last but not least, the AC signal is supplied to the cell via cables having inductance L_{cab}, which may give quite substantial contribution to the measured impedance at high frequencies. Summing all contributions, for the system impedance Z_{sys} we finally get

$$Z_{sys} = Z_{CCL} + i\omega L_{cab} + R_m \tag{8}$$

For the reasons discussed below, R_m in Eq. (8) must be prescribed in advance. Fitting of Eq. (8) to the measured impedance gives four fitting parameters: σ_p, σ_e, C_{dl}, and L_{cab}.

3. Experimental

The PGM-free catalysts were synthesized by previously reported method [16], and can be briefly described here as: transition metal nitrate/s (iron or manganese) was mixed with high surface area silica (SA = 400 m^2 g^{-1}) and organic precursor using a wet mixing. The slurry was dried at T = 80 °C for 8 h and heat treated in nitrogen atmosphere at T = 1000 °C for 90 min. The obtained powder was immersed into 25 wt% solution of HF for 48 h, filtrated and dried at T = 80 °C for 8 h. The second heat treatment was done in nitrogen atmosphere at T = 1025 °C for 45 min. The variations in synthesis were: sample N2LSA in addition to the organic material Urea was added, sample N2LDF contains addition of manganese to the iron (Fe-Mn-N-C) and N2PNN is a N2LSA catalyst which was heat treated after HF leaching step in ammonia instead of nitrogen. The CCMs from prepared catalysts were manufactured at IRD Fuel Cells, LLC using proprietary digital spray coating method.

Membrane-electrode assemblies (MEAs) with active area size of 23 cm^2 were tested at 80 °C using a cell hardware manufactured by Fuel Cell Technology Inc. The anode and cathode were fed with H_2 and N_2 respectively, at constant flow rates of 0.5 slpm at 100% relative humidity and 150 kPa absolute backpressure for both electrodes. EIS measurements were performed under potentiostatic control of the cell voltage and in two-electrode configuration, when counter and reference electrodes were connected to the anode, while working and sense electrodes to the cathode. The cathode potential was set at 0.5 V vs the anode potential (the cell anode at 0 V was used as reference and counter electrode). The cell anode works as hydrogen evolving electrode and the AC voltage perturbation was applied to the cell cathode. The amplitude of perturbation voltage signal was 10 mV, and a frequency range from 10 kHz to 0.1 Hz was chosen. Measurements were performed with 20 st/dec for frequencies from 10 kHz to 10 Hz and 10 st/dec for 10 to 0.1 Hz.

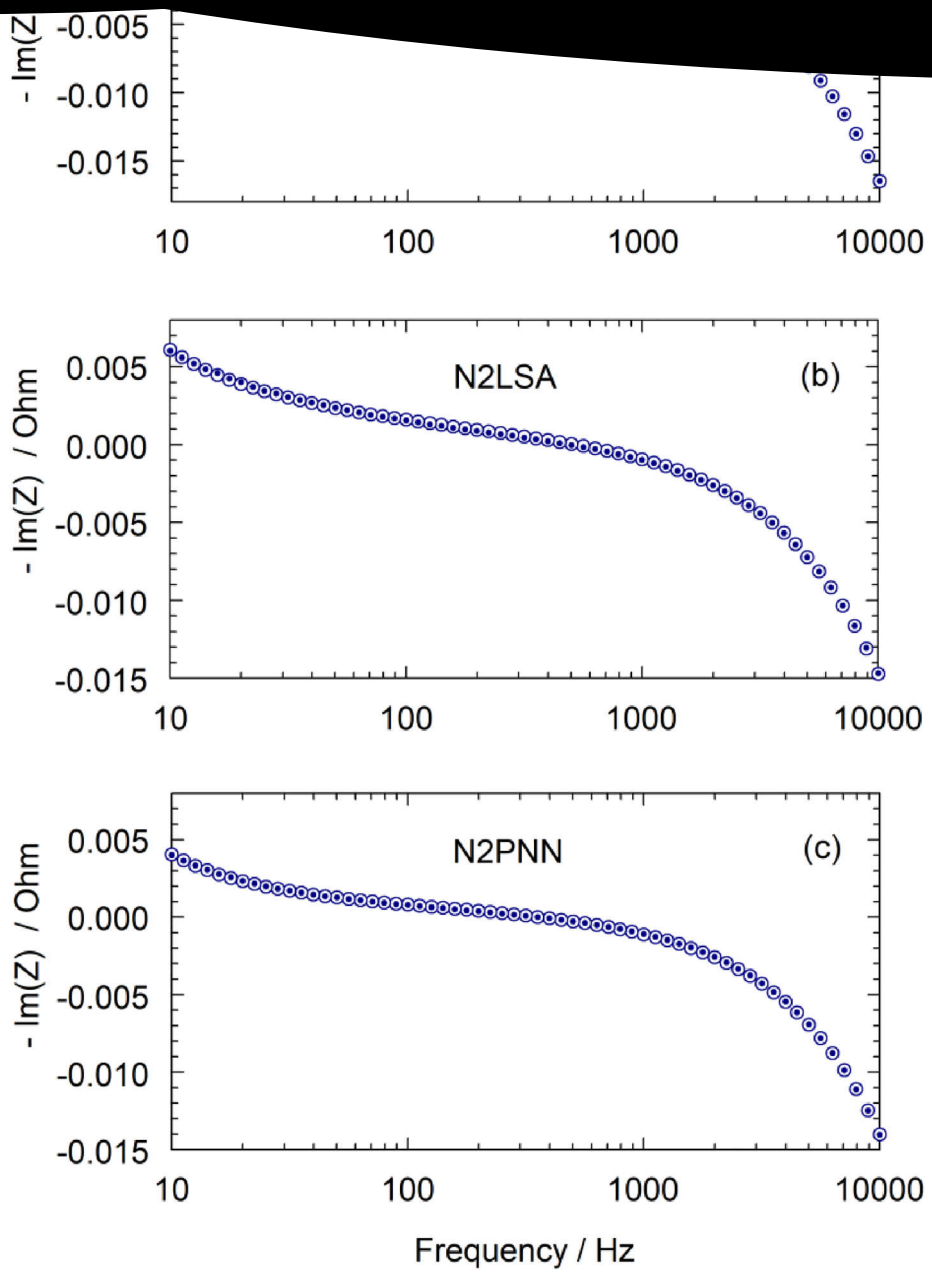

Fig 1. Experimental (points) and fitted model (open circles) frequency dependence of imaginary part of cell impedance.

4. Results and discussion

Preliminary fitting of the Nyquist spectra has revealed the following problem. The intercept of the Nyquist plot with the real axis (high frequency resistance, HFR) represents the sum of three resistances in series: the proton resistance of the membrane, the electronic resistance of the cell hardware, and the high–frequency resistance of the CCL given by Eq. (7). The fitting procedure was not able to distinguish the membrane/electronic resistance R_m and the HFR resistance of the CCL. An attempt to claim R_m in Eq. (8) as a fitting parameter have led to unrealistically low values of R_m. To resolve the problem, imaginary part of Eq. (8) has been fitted to imaginary part of experimental impedance as $\mathrm{Im}(Z_{sys})$ does not contain pure ohmic contributions. Fitting has been performed using a custom Python code and the *least_squares* subroutine from SciPy library. Measured points in the frequency range from 10 to 10000 Hz have been used for fitting. Below 10 Hz the model does not fit the experimental spectra well, seemingly due to contribution of carbon corrosion faradaic impedance not described by Eq. (8).

Experimental and fitted model H_2/N_2 frequency dependencies of imaginary part of impedance of the three samples are shown in Fig. 1. All the three spectra are fitted very well. The parameters resulted from fitting are listed in Table 1. Overall, the proton conductivity is close to the typical conductivity of standard Pt/C electrodes (5–30 mS cm^{-1} [17,18]). σ_p around 20 mS cm^{-1} exhibited by the electrodes N2LDF and

Double layer capacitance C_{dl}, F cm	13.3		
Cable inductivity L_{cab}, mH	0.265	0.237	

N2LSA is close to proton conductivity of the Fe-N-C based cell operating in H_2/air regime at the current densities below 75 mA cm^{-2} [19]. Twice higher proton conductivity of the sample N2PNN is seemingly due to higher ionomer content.

Much less is known about electron conductivity of Fe-N-C cathodes. Fitting gives σ_e in the range of 100 to 1000 mS cm^{-1} (Table 1). These values fall into the range of 100 to 2000 mS cm^{-1} for Pt/C electrodes reported by Suzuki et al. [1], though the structure of carbon cluster in Fe-N-C systems may differ from that structure in Pt/C cathodes.

Variation of the volumetric double layer capacitance C_{dl} between the three electrodes is not large (13 to 20 F cm^{-3}). This value agrees well with the impedance measurements of this parameter in a working cell at low currents [19]. C_{dl} values are also confirmed by recent publications, where measurements were conducted on CCLs fabricated with a similar Fe-N-C catalysts [20,21].

The order of magnitude of the σ_p values obtained by our model fitting correspond to data recently reported in the literature for CCLs fabricated with similar catalysts [20,21]. Considering that the proton conductivity within an electrode depend on several factors such as ionomer content, catalyst loading, ink solvent, ink deposition method, RH of measurement, these results confirm the goodness of our model. It is worth noting close values of the cable inductance (around 0.24 mH) returned by the fitting procedure in all the three measurements (Table 1).

The characteristic frequency of proton transport is proportional to the CCL proton conductivity. As this conductivity is unknown in advance, fitting requires careful selection of the low—frequency cutoff f_{LF} of the measured points used for fitting. Our strategy was to take f_{LF} as small as possible based on the quality of fitting the Nyquist spectrum of Eq. (8) to the experiment. Note that generally, the best strategy for measuring σ_p and σ_e would be fitting of the Nyquist spectra provided that the membrane/electronic resistance R_m is known from independent measurements.

In H_2/N_2 mode, current in the Pt/C-based cell arises due to oxidation of hydrogen penetrated through the membrane to the cell cathode, while in the Fe-N-C-based cell this current is most probably due to carbon corrosion on the cell cathode. However, in spite of quite different sources of current, the method above is suitable for measuring cathode electron and proton conductivity in cells of both types. In particular, the model-based impedance measurements of σ_e might be useful for control of carbon support state in long-term cell or stack operation. It is worth mentioning that the software supplied with modern EIS-meters allows to code user-defined functions for the cell impedance and simple Eq. (8) can be used for this purpose.

5. Conclusions

We report a method for simultaneous *in-situ* measurement of proton and electron conductivity of the Pt/C and PGM-free cathode catalyst layer in PEM fuel cells. Experimental impedance spectra of the cell operating in H_2/N_2 regime are fitted using a recent impedance model, which takes into account finite proton σ_p and electron σ_e conductivity of the CCL. The method consists of the following steps:

1. Measuring the cell impedance in H_2/N_2 mode
2. Fitting of the function $\mathrm{Im}(Z_{CCL}) + \omega L_{cab}$ to the measured imaginary

of electron co
of carbon support corrosion during long-term cell operation.

CRediT authorship contribution statement

Tatyana Reshetenko: Conceptualization, Investigation, Validation, Writing - original draft. **Alexey Serov:** Supervision, Conceptualization, Methodology, Investigation, Writing - original draft. **Madeleine Odgaard:** Investigation, Resources. **Günter Randolf:** . **Luigi Osmieri:** Conceptualization, Methodology, Writing - original draft. **Andrei Kulikovsky:** Conceptualization, Methodology, Supervision, Writing - original draft, Software.

Declaration of Competing Interest

The authors declare that they have no known competing financial interests or personal relationships that could have appeared to influence the work reported in this paper.

Acknowledgements

TR, AS, MO gratefully acknowledge financial support from US DOE EERE (DE-EE0008419 “Active and Durable PGM-free Cathodic Electrocatalysts for Fuel Cell Application”). TR gratefully acknowledges funding from US Office of Naval Research (N00014-19-1-2159).

This work was authored in part by Alliance for Sustainable Energy, LLC, the manager and operator of the National Renewable Energy Laboratory for the U.S. Department of Energy under Contract No. DE-AC36-08GO28308. The views expressed in the article do not necessarily represent the views of the DOE or the U.S. Government.

References

[1] T. Suzuki, H. Murata, T. Hatanaka, Y. Morimoto, R&D Rev. Toyota CRDL. 39 (2003) 33–38.
[2] S.T. Thompson, A.R. Wilson, P. Zelenay, D.J. Myers, K.L. More, K.C. Neyerlin, D. Papageorgopoulos, Solid State Ionics. 319 (2018) 68–76, https://doi.org/10.1016/j.ssi.2018.01.030.
[3] Y. He, S. Liu, C. Priest, Q. Shi, G. Wu, Chem. Soc. Rev. (2020) 3484–3524, https://doi.org/10.1039/c9cs00903e.
[4] U. Tylus, Q. Jia, K. Strickland, N. Ramaswamy, A. Serov, P. Atanassov, S. Mukerjee, J. Phys. Chem. C. 118 (2014) 8999–9008, https://doi.org/10.1021/jp500781v.
[5] J. Li, F. Jaouen, Curr. Opin. Electrochem. 9 (2018) 198–206, https://doi.org/10.1016/j.coelec.2018.03.039.
[6] K. Artyushkova, M.J. Workman, I. Matanovic, M.J. Dzara, C. Ngo, S. Pylypenko, A. Serov, P. Atanassov, A.C.S. Appl, Energy Mater. 1 (2018) 68–77, https://doi.org/10.1021/acsaem.7b00002.
[7] A. Serov, M.J. Workman, K. Artyushkova, P. Atanassov, G. McCool, S. McKinney, H. Romero, B. Halevi, T. Stephenson, J. Power Sources. 327 (2016) 557–564, https://doi.org/10.1016/j.jpowsour.2016.07.087.
[8] S. Rojas-Carbonell, K. Artyushkova, A. Serov, C. Santoro, I. Matanovic, P. Atanassov, ACS Catal. 8 (2018) 3041–3053, https://doi.org/10.1021/acscatal.7b03991.
[9] F. Jaouen, D. Jones, N. Coutard, V. Artero, P. Strasser, A. Kucernak, Johnson Matthey Technol. Rev. 62 (2018) 231–255, https://doi.org/10.1595/205651318X696828.
[10] K.C. Neyerlin, W. Gu, J. Jorne, A. Clark, H.A. Gasteiger, J. Electrochem. Soc. 154 (2007) B279–B287, https://doi.org/10.1149/1.2400626.
[11] C.Y. Du, P.F. Shi, X.Q. Cheng, G.P. Yin, Electrochem. Commun. 6 (2004) 435–440, https://doi.org/10.1016/j.elecom.2004.02.006.
[12] M. Ahadi, M. Tam, J. Stumper, M. Bahrami, Int. J. Hydrogen Energy. 44 (2019) 3603–3614, https://doi.org/10.1016/j.ijhydene.2018.12.016.
[13] Z. Tang, Q.A. Huang, Y.J. Wang, F. Zhang, W. Li, A. Li, L. Zhang, J. Zhang, J. Power Sources. 468 (2020) 228361, , https://doi.org/10.1016/j.jpowsour.2020.228361.
[14] A. Kulikovsky, J. Electroanal. Chem. 801 (2017) 122–128, https://doi.org/10.1016/j.jelechem.2017.07.038.

[18] L. Liu, Z. Liang, H. Cheng, Y. Liang, Q. Tan, Cr
Crossover in DMFC, (2009) 43–51. doi:10.1149/1.3248348.